

Determine the quantum numbers of $X(6900)$ from photon-photon fusion in ultra-peripheral heavy ion collisions

Peng-Yu Niu,^{1,2,*} Enke Wang,^{1,2,†} Qian Wang,^{1,2,‡} and Shuai Yang^{1,2,§}

¹*Guangdong Provincial Key Laboratory of Nuclear Science, Institute of Quantum Matter,
South China Normal University, Guangzhou 510006, China*

²*Guangdong-Hong Kong Joint Laboratory of Quantum Matter,
Southern Nuclear Science Computing Center, South China Normal University, Guangzhou 510006, China*
(Dated: September 7, 2022)

We study the production of the $X(6900)$ through the $J/\psi J/\psi$ decay channel in the ultra-peripheral heavy ion collisions at the LHC energy region. The potential quantum numbers of $X(6900)$ would be $0^{\pm+}$ and $2^{\pm+}$. We find that the transverse momentum and the polar angle distributions of $X(6900)$ can be used to distinguish these four potential quantum numbers. These typical distributions stem from the linearly polarized photon from the fast-moving nuclei and can be measured with the LHC experiments in further.

PACS numbers:

I. INTRODUCTION

Over the past two decades, a large number of exotic states, which are not compatible with $q\bar{q}$ or qqq of the traditional quark model states, have been discovered. Recently, the LHCb Collaboration reported resonance-like structures in the J/ψ -pair invariant mass distribution [1, 2] in p+p collisions at center-of-mass energies of $\sqrt{s} = 7, 8, 13$ TeV, corresponding to an integrated luminosity of 9 fb^{-1} . A narrow structure around 6.9 GeV, so-called $X(6900)$, and a broad structure slightly above the $J/\psi J/\psi$ threshold were reported. Considering their mass positions and the observed channels, the community reach a consensus that they contain two charm and two anti-charm quarks. Later on, the CMS Collaboration [3] reported three resonance-like structures through the same channel in p+p collisions at $\sqrt{s} = 13$ TeV with an integrated luminosity of 135 fb^{-1} . The significances of the lower two structures with mass of $6927 \pm 9 \pm 5 \text{ MeV}$ and $6552 \pm 10 \pm 12 \text{ MeV}$ are well above 5 standard deviations. The highest structure with a mass of $7287 \pm 19 \pm 5 \text{ MeV}$ is with a significance of 4.1 standard deviation. The first one is consistent with the $X(6900)$ reported by the LHCb Collaboration. Meanwhile, the ATLAS Collaboration [4] also reported similar structures. Those structures are the first measurements of full-charm tetraquarks, arising intensive discussions among the hadron physics community. The $X(6900)$ can be accepted by both compact tetraquark [5–19] and hadronic molecular pictures [20–22]. It can be either a pseudoscalar P -wave state with $J^{PC} = 0^{-+}$ or a scalar S -wave state with $J^{PC} = 0^{++}$ [13, 23–30]. Another possible quantum number scenario might be $J^{PC} = 2^{++}$ as discussed in Refs. [5–8, 26–32]. In the molecular picture, both $J^{PC} = 0^{-+}$ and $J^{PC} = 2^{++}$ are allowed [20, 21]. Therefore, the determination of its quantum numbers, especially a distinguish between 0^{-+} and 0^{++} would shed new light on the nature of these recently measured full-charm tetraquark states.

On the other hand, the Lorentz-boosted electromagnetic fields surrounding ultrarelativistic heavy ions with large charges can be treated a flux of quasireal photons[33–35]. The photon intensity is proportional to the square of the ion charge (Z). Exclusive photon-photon interactions, especially the $\gamma\gamma \rightarrow l^+l^-$ processes, have been extensively studied in ultra-peripheral and hadronic heavy ion collisions [36–55]. Moreover, photon-photon interactions can be used to study the exotic particles [56–61], Higgs bosons [62–65], and to search for physics beyond the standard model [66–69]. Recently, people realized that the equivalent photon has impact parameter (b) dependence [55, 70–73] and is linearly polarized [74, 75]. Specifically, the linear polarized photons lead to the $\cos(4\phi)$ azimuthal asymmetry for dilepton production from photon-photon scatterings, confirmed by the STAR Collaboration [51]. This linearly polarized quasireal photons could provide an extra information about the spin of particle created by photon-photon fusion. In ultra-peripheral collisions (UPC), the nuclei pass on another with an impact parameter greater than twice the nuclear radius, which means no nuclear overlap occurs. Based on this facts, UPC provides an excellent platform

*Electronic address: niupy@m.scnu.edu.cn

†Electronic address: wangek@scnu.edu.cn

‡Electronic address: qianwang@m.scnu.edu.cn

§Electronic address: syang@scnu.edu.cn

to investigate the exotic states created by photon-photon fusion with the following advantages: 1) the background is significantly suppressed compared with that in hadronic collisions, 2) the cross section is enhanced by Z^4 compared with that in e^+e^- collisions.

In this work, we focus on the $X(6900)$ kinematic distributions instead of absolute cross section to determine its quantum numbers, which could be 0^{++} , 0^{-+} , 2^{++} and 2^{-+} . We demonstrate that the kinematic distributions provide a powerful tool to identify the quantum numbers of $X(6900)$ in the future measurements at the LHC. This paper is organized as follows. Sec. II describes the details of calculation. The results and discussions are presented in details in Sec. III. Lastly, Sec. IV provides a concluding summary.

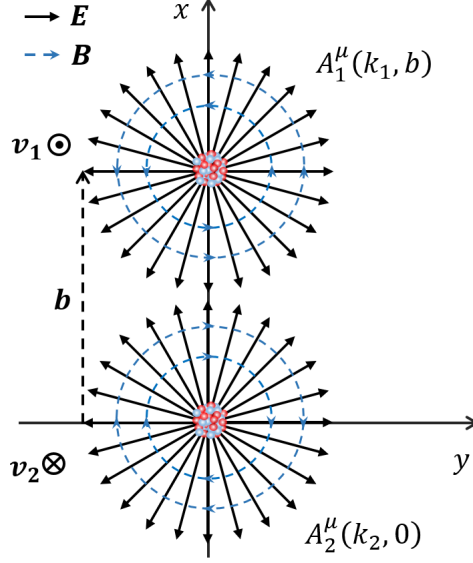


FIG. 1: Illustration of the electric and magnetic field lines in the plane perpendicular to the beam. The black solid and blue dashed lines are for electric and magnetic fields, respectively. v_1 and v_2 are velocities of the two nuclei. b is the impact parameter defined as the distance between the two nuclei in the transverse plane with respect to the beam.

II. FRAMEWORK

The electromagnetic field surrounding ultra-relativistic nuclei are highly contracted and nearly perpendicular to the direction of motion, as depicted in Fig. 1. Therefore, the photons generated by these fields are expected to be linearly polarized in the transverse plane with respect to the beam [74, 75]. The electromagnetic fields of the two nuclei are treated classically. The two nuclei are approximated to move with constant velocity on straight lines with an impact parameter b as shown in Fig. 2, with negligible deflections due to the collision. Accordingly, the two electromagnetic potentials read as [70],

$$A_1^\mu(k_1, \mathbf{b}_1) = -2\pi Z_1 e \delta(k_1 \cdot u_1) \frac{F(-k_1^2)}{k_1^2} e^{ik_1 \cdot b_1} \times u_1^\mu, \quad (1)$$

$$A_2^\mu(k_2, \mathbf{b}_2) = -2\pi Z_2 e \delta(k_2 \cdot u_2) \frac{F(-k_2^2)}{k_2^2} e^{ik_2 \cdot b_2} \times u_2^\mu, \quad (2)$$

where δ function ensures that the nuclei moves along a straight line with a constant velocity. k_1 and k_2 are the four momenta of the two photons, respectively. $u_1 = \gamma(1, 0, 0, -v)$ (Z_1) and $u_2 = \gamma(1, 0, 0, +v)$ (Z_2) are the four velocities (nuclear charge numbers) of the two nuclei, respectively. $\gamma = (1 - v^2)^{-1/2}$ is the Lorentz contraction factor. $\mathbf{b}_1 = (b, 0, 0)$ and $\mathbf{b}_2 = (0, 0, 0)$ are the coordinates of the two nuclei. $F(-k_1^2)$ and $F(-k_2^2)$ are the charge form factors of two nuclei, which is the Fourier transform of its spatial charge distribution of the nucleus, as shown in Eq. 3

$$F(k^2) = \int d^3\mathbf{r} \rho(\mathbf{r}) e^{i\mathbf{k} \cdot \mathbf{r}} \quad (3)$$

TABLE I: The employed values of the skin depth d and the radius R_{WS} of Au and Pb.

| | Ref. [81] | | Ref. [71, 74] | |
|------------|-----------|------|---------------|-------|
| | Au | Pb | Au | Pb |
| d [fm] | 0.41 | 0.45 | 0.535 | 0.546 |
| R_A [fm] | 6.42 | 6.66 | 6.38 | 6.62 |

Here \mathbf{k} and \mathbf{r} are momentum and coordinate, respectively. For a high- Z nucleus, the spatial charge distribution in rest frame is well described by the Woods-Saxon distribution [76]:

$$\rho(r) = \frac{\rho_0}{1 + \exp[(r - R_A)/d]}, \quad (4)$$

where ρ_0 is the normalization factor. r is the distance between a given point and the nucleus center. d and R_A are the skin depth and the radius of a nucleus, respectively. The employed values of those two parameters in this work are summarized in Tab. I. However, it is hard to perform the Fourier transform analytically to obtain $F(k^2)$. Alternatively, an approximation

$$F(|k|) = \frac{4\pi\rho_0}{A|k^3|} \left(\frac{\sin(|k|R_A) - |k|R_A \cos(|k|R_A)}{1 + a^2 k^2} \right) \quad (5)$$

is widely employed in literatures [77]. Here A is the mass number of nucleus and $R_A = 1.1A^{1/3}$ fm is the radius of Woods-Saxon distribution with a hard sphere [74] ($R_A = 1.2A^{1/3}$ fm is also used in Refs. [64, 78]). a is the Yukawa potential range which is characterized by the inverse of the pion mass, i.e. 0.7 fm [79]. ρ_0 is also considered as a normalization factor, ensuring $F(0) = 1$.

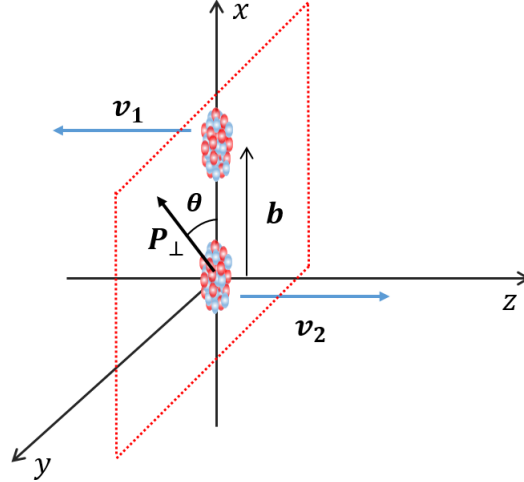


FIG. 2: The setup of the coordinate for the photo-photon fusion process in UPC. v_1 and v_2 are the velocities of two nuclei. The z -axis is chosen along beam direction. The direction of the nucleus-nucleus impact parameter \vec{b} points from one nucleus to another, e.g. from nucleus with velocity v_2 to nucleus with velocity v_1 , also serving as the direction of the x -axis. Thus, the y -axis can be determined by right hand rule.

A Feynman-like diagram for the production of the X in photon-photon fusion process is shown in Fig. 3. For photon-photon fusion process, the nuclei can be assumed to move along straight lines and their deflection can be neglected, as the transverse momentum is much smaller than the longitudinal momentum. Therefore, the emitted photon fields can be treated as EM external fields, and the production amplitude can be expressed as [70]

$$\begin{aligned} \mathcal{M}(k_1, k_2, P) &= \int \frac{d^4 k_1}{(2\pi)^4} \frac{d^4 k_2}{(2\pi)^4} [A_1^\mu(k_1, b) \Gamma_{\mu\nu}(k_1, k_2) A_2^\nu(k_2, 0)] (2\pi)^4 \delta^4(k_1 + k_2 - P) \\ &= Z^2 \frac{e^2}{\gamma^2} \int \frac{d^4 k_1}{(2\pi)^2} \delta(k_1^0 - vk_1^3) \delta(P^0 + vP^3 - k_1^0 - vk_1^3) \frac{F(-k_1^2)}{-k_1^2} \frac{F(-k_2^2)}{-k_2^2} u_1^\mu u_2^\nu \Gamma_{\mu\nu}(k_1, k_2) e^{-i\mathbf{b} \cdot \mathbf{k}_{1,\perp}} \\ &= Z^2 \frac{e^2}{2v\gamma^2} \int \frac{d^2 \mathbf{k}_{1,\perp}}{(2\pi)^2} \frac{F(-k_1^2)}{-k_1^2} \frac{F(-k_2^2)}{-k_2^2} u_1^\mu u_2^\nu \Gamma_{\mu\nu}(k_1, k_2) e^{-i\mathbf{b} \cdot \mathbf{k}_{1,\perp}} \Big|_{k_2=P-k_1}, \end{aligned} \quad (6)$$

where $P = (P^0, \mathbf{P}_\perp, P^3)$ is the four momentum of the produced X particle. Here the subscript “ \perp ” is used to label the transverse component and $\mathbf{P}_\perp = (P^1, P^2)$. $\delta^4(k_1 + k_2 - P)$ is the requirement of the four momentum conservation. $\Gamma_{\mu\nu}$ is the vertex function which depends on the quantum number of created particles and will be discussed in details later. The two photon momenta k_1 and k_2 read as

$$k_1 = (\omega_1, \mathbf{k}_\perp, \omega_1/v), \quad k_2 = (\omega_2, \mathbf{P}_\perp - \mathbf{k}_\perp, -\omega_2/v), \quad (7)$$

with $\omega_1 = 1/2(P_0 + vP_z)$ and $\omega_2 = 1/2(P_0 - vP_z)$ the energies of the 1st and 2nd photons, respectively. Because the transverse momentum is much smaller than the longitudinal momentum, the two photons can be approximately on-shell. $\omega_{1,2}$ and \mathbf{k}_\perp is the integration variable. Considering that $|\mathbf{k}_\perp|_{\min} = 0$, k_1 and k_2 are space-like vectors, for instance

$$k_1^2 = \omega_1^2 - \mathbf{k}_{1\perp}^2 - \omega_1^2/v^2 \leq \omega_1^2 - \omega_1^2/v^2 \approx -\left(\frac{\omega_1}{\gamma}\right)^2. \quad (8)$$

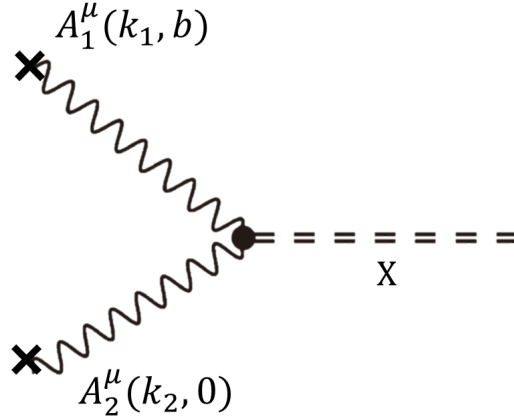


FIG. 3: A Feynman-like diagram for the production of the X with two classical external fields $A_{1,2}^\mu$

In e^+e^- collisions, the deflection of the scattering electron or positron leads to finite virtuality of the emitted photon. In contrary, the heavy ions maintain their straight-line trajectory in UPC. Thus, the low-energy photon is regulated by the finite Lorentz contraction factor γ of the ions, i.e. $|k^2| \geq (\omega/\gamma)^2$ with ω the photon energy, avoiding singularity in Eq. (6). The high-energy photon is naturally cut off by the finite size of the ion's charge distribution, i.e. $|k^2| \leq (1/R_A)^2$, in which R_A is the nuclear radius [70]. Those are consistent with Eq. (8). For a given nucleus, the transverse momentum of photon is constrained by $k_\perp^2 \leq 1/R_A^2 - (\omega/\gamma)^2$.

In this paper, we consider the production of hadrons with all the possible quantum numbers, i.e. $0^{\pm+}$ and $2^{\pm+}$, in photon-photon fusion process. Hadrons with spin-1 cannot be produced due to Landau-Yang theorem [82]. For scalars [70] and pseudoscalars, the vertex functions are

$$\Gamma_{\mu\nu}^{0^{++}} = g_s(k_1 \cdot k_2 g_{\mu\nu} - k_{1\nu} k_{2\mu}), \quad (9)$$

$$\Gamma_{\mu\nu}^{0^{-+}} = g_{sp} \epsilon_{\mu\nu\alpha\beta} k_1^\alpha k_2^\beta, \quad (10)$$

respectively. k_1 and k_2 are four momenta of the two photons. g_s and g_{sp} are the corresponding effective couplings. The vertex functions for $2^{\pm+}$ hadrons are

$$\Gamma_{\mu\nu}^{2^{++}} = g_t (g_{\mu\nu} k_{1\rho} k_{2\sigma} \epsilon^{\rho\sigma} + k_1 \cdot k_2 \epsilon^{\mu\nu} - k_{1\mu} k_{2\rho} \epsilon^{\rho\nu} - k_{2\mu} k_{1\rho} \epsilon^{\rho\nu}), \quad (11)$$

and

$$\Gamma_{\mu\nu}^{2^{-+}} = g_{tp} \epsilon_{\mu\lambda\alpha\beta} k_1^\alpha k_2^\beta \epsilon_\nu^\lambda. \quad (12)$$

The polarized vector of spin-2 particle reads as

$$\epsilon_{\mu\nu}(\vec{p}, \lambda) = \sum_{\lambda_1, \lambda_2} \langle 1\lambda_1; 1\lambda_2 | 2\lambda \rangle \epsilon_\mu(\vec{p}, \lambda_1) \epsilon_\nu(\vec{p}, \lambda_2) \quad (13)$$

with λ indicating the third component of spin. \vec{p} is the three momentum of the produced tensor. If the vertex function $\Gamma_{\mu\nu}$ contracts with two real photons, it is easy to verify that the amplitudes satisfy gauge invariance. With all the amplitude ready, one can obtain the differential cross section[70]

$$d\sigma = d^2\mathbf{b} |\mathcal{M}(k_1, k_2, P)|^2 \frac{d^4P}{(2\pi)^4} d\alpha, \quad (14)$$

where $d\alpha$ is the n-body phase space

$$d\alpha = \delta^4(P - \sum_{i=1}^n p_i) \frac{d^3\mathbf{p}_1}{(2\pi)^3 2E_1} \frac{d^3\mathbf{p}_2}{(2\pi)^3 2E_2} \cdots \frac{d^3\mathbf{p}_n}{(2\pi)^3 2E_n}. \quad (15)$$

In this paper, only one-body phase space should be considered. Thus, the differential cross section can be simplified to the following form:

$$\sigma = \frac{2}{(2\pi)^3 2|P_z|} \int d^2\mathbf{b} |\mathcal{M}(k_1, k_2, P)|^2 dP_0 d^2\mathbf{P}_\perp \theta(E_0) |_{P_z = \sqrt{P_0^2 - \mathbf{P}_\perp^2 - M_X^2}}, \quad (16)$$

where M_X is the mass of hadron X . As the effective couplings g_s, g_{sp}, g_t and g_{tp} are not determined yet, the total cross section cannot be accurately predicted. The cross section of the $X(6900)$ in photon-photon fusion process has been estimated by Vector Meson Dominance model in Ref. [61]. This work focuses on the transverse momentum P_\perp distribution $d\sigma/(dP_\perp)$ and the polar angle distribution $d\sigma/(d\theta)$ of $X(6900)$, which can be used to distinguish various quantum numbers. Those two distributions can be obtained by integrating out another dimension from

$$\frac{d\sigma}{d|P_\perp| d\theta} \propto \int d^2\mathbf{b} dP_0 |\mathbf{P}_\perp| |\mathcal{M}(k_1, k_2, P)|^2 |_{P_z = \sqrt{P_0^2 - \mathbf{P}_\perp^2 - M_X^2}}, \quad (17)$$

where θ is the azimuth angle of \mathbf{P}_\perp as illustrated by Fig. 2. Because the value of total transverse momentum \mathbf{P}_\perp is small in UPC, P_z is treated as a constant number in the last step.

III. RESULTS AND DISCUSSIONS

The collision time of UPC is about $t_{\text{coll}} = R_A/\gamma$, and the maximum energy of the photon is about $\omega_{\text{max}} \approx \gamma/R_A$ [70] due to the uncertainty principle. Taking the Pb beam with the energy per nucleon $\sqrt{s_{NN}} = 5.628$ TeV as an example, the maximum photon energy can reach ~ 90 GeV with $\gamma = 3000$ and $R_A = 6$ fm [48]. Such a large energy can produce hadron with a mass as large as the $X(6900)$ discussed in Sec. I. The production of the $X(6900)$ has been studied in heavy ion collision [60, 61]. In principle, the photon energy should be integrated out to estimate the cross section of the $X(6900)$. However, we have checked that the transverse momentum P_\perp and the polar angle θ distributions, which essentially help to pin down the quantum numbers of the interested hadrons, is not sensitive to the two-photon center-of-mass energy $\sqrt{s_{\gamma\gamma}}$ in UPC (hereafter $\sqrt{s_{\gamma\gamma}}$ will be abbreviated as \sqrt{s}). So, in this work, \sqrt{s} is set to 20 GeV as an illustration. The lower limit and upper limit of the impact parameter $b = |\mathbf{b}|$ are twice nuclei radius and $+\infty$, respectively. Since the cross section decreases dramatically with the increasing b [70], the upper limit of the impact parameter b is set to be 200 fm. We have checked that when this value increases to be 300 fm and 400 fm, our results do not change. In addition, the upper limit of $|\mathbf{k}_{1\perp}|$ is set to 0.05 GeV which is larger than the value used in Refs. [48, 70, 78]. With all the parameter constraints imposed, we can obtain the P_\perp and θ distributions from Eq. (17) for all the possible quantum numbers, i.e. $J^{PC} = 0^{\pm+}$ and $J^{PC} = 2^{\pm+}$.

The differential $\frac{d\sigma}{dP_\perp}$ and $\frac{d\sigma}{P_\perp dP_\perp}$ distributions with polar angle θ and the impact parameter b integrated out, are presented in Fig. 4. In Fig. 4(b), the states with negative parity goes to zero faster than those with positive parity around $P_\perp = 0$. That is because the anti-symmetric tensor in the vertex function for the states with negative parity contracts with the photon momenta and the polarization vector/tensor of a given state. When $\mathbf{P}_\perp = 0$, $k_{1\perp}$ and $k_{2\perp}$ are symmetric, i.e. $\mathbf{k}_{1\perp} = -\mathbf{k}_{2\perp}$, and the amplitudes of the 0^- and 2^- states obviously go to zero. That is the reason why the differential P_\perp distributions go to zero faster than those with positive parity. This can be used to distinguish the states with different parities. One can also see in Fig. 4 that the differential P_\perp distributions of the same parity states have similar behavior because of the similar structure of the vertex function. While the four curves also share the same characteristic that the differential cross section decreases with the large increasing P_\perp .

We borrow the idea for the oscillation behavior of the dilepton pair distribution in UPC [74, 75, 83] and also present the differential polar angle θ distributions in Fig. 5. They oscillate with the period π for all the cases. There is no doubt that the system is symmetric with respect to the plane the two heavy ions locate at, i.e. the $x - z$ plane

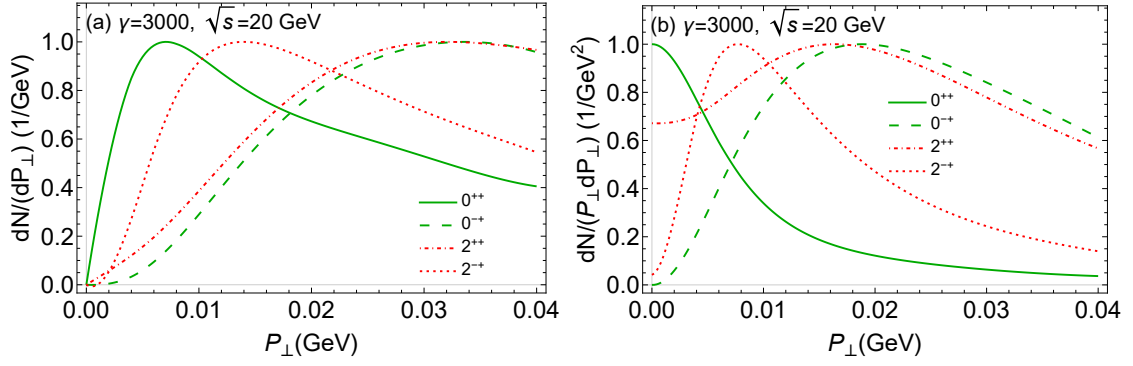


FIG. 4: The differential $\frac{d\sigma}{dP_{\perp}}$ (panel a) and $\frac{d\sigma}{P_{\perp} dP_{\perp}}$ (panel b) distributions with polar angle θ and the impact parameter b integrated out. As all the effective couplings g_s, g_{sp}, g_t, g_{tp} are not determined, all the curves are rescaled to make the largest value to be one. The green solid and green dashed curves are for the 0^{++} and 0^{-+} states, respectively. The red dot-dashed and the red dotted curves are for the 2^{++} and 2^{-+} states, respectively.

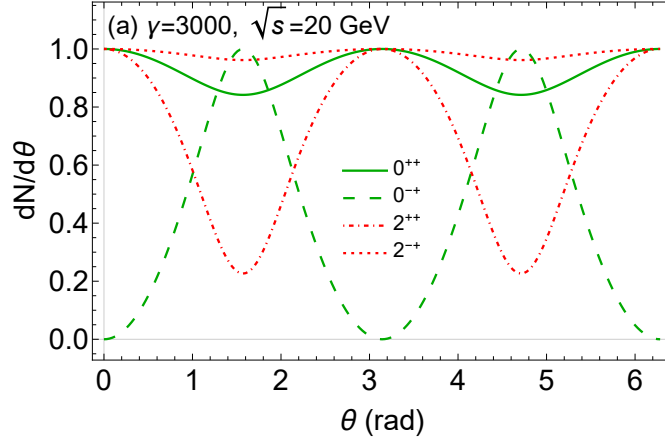


FIG. 5: The differential polar angle θ distributions with the transverse momentum \mathbf{P}_{\perp} and the impact parameter b integrated out. All the curves are also rescaled to make their large values to be one. The labels of the four curves have the same meaning as those in Fig. 4.

in Fig. 2. The 0^+ , 2^+ , 2^- distributions are “W”-type and the 0^- distribution is “M”-type. This can be used to distinguish the 0^- quantum number from the others. The oscillation strengths of the 0^- and 2^+ states are larger than those of the other two scenarios.

Fig. 6 shows the differential polar angle θ distributions for the transverse momentum regions $(0.00, 0.01]$, $(0.01, 0.02]$, $(0.02, 0.03]$, $(0.03, 0.04]$, and $(0.04, 0.05]$ GeV. The 0^{-+} and 2^{++} states oscillate more significant than the 0^{++} and 2^{-+} states, which has already been seen from Fig. 5. The 0^{-+} distributions for all the P_{\perp} regions are “M” type, and the distributions for other states for all the P_{\perp} regions are “W” type. The oscillation for the 2^{++} state is more significant than those of the 0^{++} and 2^{-+} states. The largest values of the 0^{++} and 2^{-+} states are the $(0.00, 0.01]$ GeV and $(0.01, 0.02]$ GeV regions, respectively. This behavior can be used to distinguish these two states.

The above distributions, which could be measured at the LHC, can be used to determine the quantum numbers of the $X(6900)$. As our framework does not depend on the property of the $X(6900)$, it cannot help to shed light on its internal structure, for instance compact tetraquark or hadronic molecule. On the other hand, our framework does not only work for the $X(6900)$, but also works for other regular and exotic hadrons.

IV. SUMMARY

Since the observation of the first full-charm tetraquark $X(6900)$, the community intensively discuss its internal structure, i.e. either compact tetraquark or hadronic molecule. For the compact tetraquark scenario, all the $J^{PC} = 0^{\pm+}$ and 2^{++} quantum numbers are allowed. However, its quantum number cannot be well established due to the

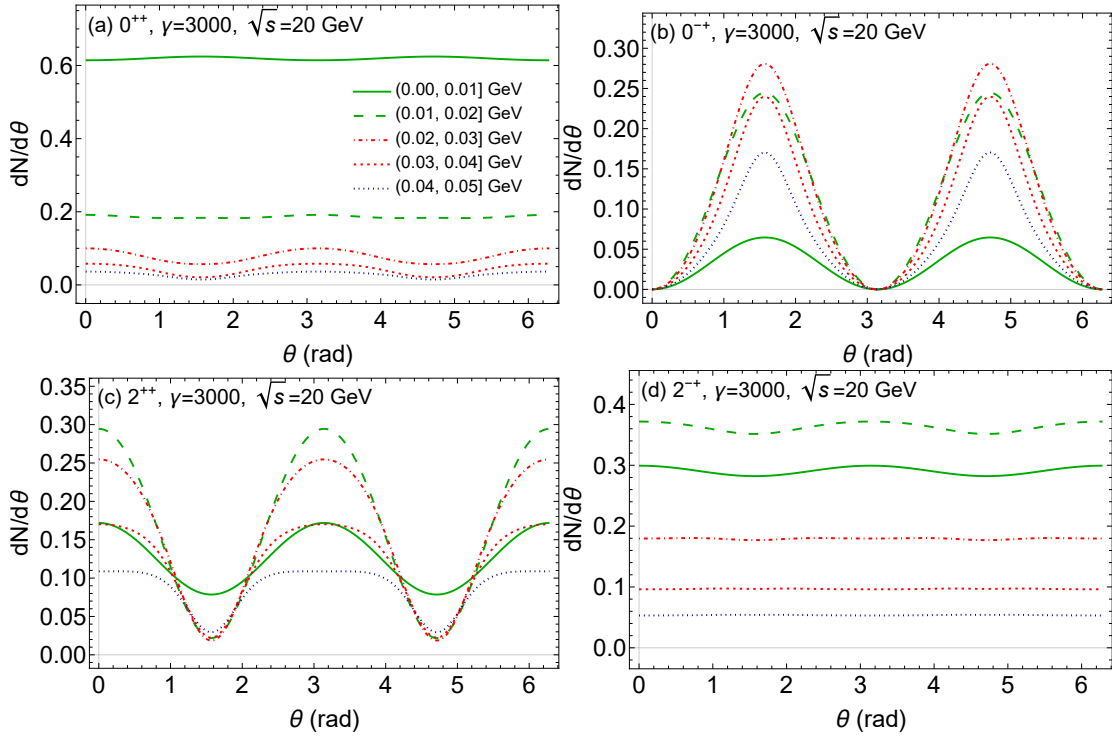


FIG. 6: The differential polar angle θ distributions for various transverse momentum regions, with the Lorentz contraction parameters $\gamma = 3000$ and the two-photon center-of-mass energy $\sqrt{s} = 20$ GeV. The green solid, green long dashed, red dot-dashed, red dashed and blue dotted curves are used to label the distributions of the transverse momentum regions (0.00, 0.01], (0.01, 0.02], (0.02, 0.03], (0.03, 0.04], and (0.04, 0.05] GeV, respectively.

low statistic in current experiments. We take advantage of the polarized photon produced in UPC and predict the transverse momentum and polar angle distributions of the $X(6900)$. These two distributions exhibit significant difference for the four potential quantum numbers $J^{PC} = 0^{\pm+}, 2^{\pm+}$, which can be used help to determine the quantum number of the $X(6900)$. As this method does not depend on the internal structure of the interested hadrons, it can also work for other hadrons with spin other than one.

Acknowledgments

The discussion with Hui Zhang is acknowledged. This work is partly supported by Guangdong Major Project of Basic and Applied Basic Research No. 2020B0301030008, the National Natural Science Foundation of China with Grant No. 12147128, No. 12035007, Guangdong Provincial funding with Grant No. 2019QN01X172. Q.W. is also supported by the NSFC and the Deutsche Forschungsgemeinschaft (DFG, German Research Foundation) through the funds provided to the Sino-German Collaborative Research Center TRR110 “Symmetries and the Emergence of Structure in QCD” (NSFC Grant No. 12070131001, DFG Project-ID 196253076-TRR 110).

-
- [1] R. Aaij *et al.* [LHCb], JHEP **10**, 086 (2018) [arXiv:1806.09707 [hep-ex]].
 - [2] R. Aaij *et al.* [LHCb], Sci. Bull. **65**, no.23, 1983-1993 (2020) [arXiv:2006.16957 [hep-ex]].
 - [3] The CMS Collaboration, “Observation of new structures in the $J/\psi J/\psi$ mass spectrum in pp collisions at $\sqrt{s} = 13$ TeV”, CMS-PAS-BPH-21-003.
 - [4] The ATLAS Collaboration, “Observation of an excess of di-charmonium events in the four-muon final state with the ATLAS detector”, ATLAS-CONF-2022-040.
 - [5] R. N. Faustov, V. O. Galkin and E. M. Savchenko, Universe **7**, no.4, 94 (2021) [arXiv:2103.01763 [hep-ph]].
 - [6] C. Deng, H. Chen and J. Ping, Phys. Rev. D **103**, no.1, 014001 (2021) [arXiv:2003.05154 [hep-ph]].
 - [7] H. X. Chen, W. Chen, X. Liu, Y. R. Liu and S. L. Zhu, [arXiv:2204.02649 [hep-ph]].
 - [8] X. Z. Weng, X. L. Chen, W. Z. Deng and S. L. Zhu, Phys. Rev. D **103**, no.3, 034001 (2021) [arXiv:2010.05163 [hep-ph]].

- [9] J. M. Richard, Sci. Bull. **65**, 1954-1955 (2020) [arXiv:2008.01962 [hep-ph]].
- [10] J. Sonnenschein and D. Weissman, Eur. Phys. J. C **81**, no.1, 25 (2021) [arXiv:2008.01095 [hep-ph]].
- [11] Z. H. Guo and J. A. Oller, Phys. Rev. D **103**, no.3, 034024 (2021) [arXiv:2011.00978 [hep-ph]].
- [12] A. V. Berezhnoy, A. V. Luchinsky and A. A. Novoselov, Phys. Rev. D **86**, 034004 (2012) [arXiv:1111.1867 [hep-ph]].
- [13] J. Wu, Y. R. Liu, K. Chen, X. Liu and S. L. Zhu, Phys. Rev. D **97**, no.9, 094015 (2018) [arXiv:1605.01134 [hep-ph]].
- [14] X. Chen, [arXiv:2001.06755 [hep-ph]].
- [15] M. S. Liu, Q. F. Lü, X. H. Zhong and Q. Zhao, Phys. Rev. D **100**, no.1, 016006 (2019) [arXiv:1901.02564 [hep-ph]].
- [16] G. J. Wang, L. Meng and S. L. Zhu, Phys. Rev. D **100**, no.9, 096013 (2019) [arXiv:1907.05177 [hep-ph]].
- [17] Z. Zhao, K. Xu, A. Kaewsnod, X. Liu, A. Limphirath and Y. Yan, Phys. Rev. D **103**, no.11, 116027 (2021) [arXiv:2012.15554 [hep-ph]].
- [18] H. X. Chen, W. Chen, X. Liu and S. L. Zhu, Sci. Bull. **65**, 1994-2000 (2020) [arXiv:2006.16027 [hep-ph]].
- [19] Z. G. Wang, Chin. Phys. C **44**, no.11, 113106 (2020) [arXiv:2006.13028 [hep-ph]].
- [20] X. K. Dong, V. Baru, F. K. Guo, C. Hanhart, A. Nefediev and B. S. Zou, Sci. Bull. **66**, no.24, 2462-2470 (2021) [arXiv:2107.03946 [hep-ph]].
- [21] X. K. Dong, V. Baru, F. K. Guo, C. Hanhart and A. Nefediev, Phys. Rev. Lett. **126**, no.13, 132001 (2021) [erratum: Phys. Rev. Lett. **127**, no.11, 119901 (2021)] [arXiv:2009.07795 [hep-ph]].
- [22] J. Z. Wang and X. Liu, [arXiv:2207.04893 [hep-ph]].
- [23] V. R. Debastiani and F. S. Navarra, Chin. Phys. C **43**, no.1, 013105 (2019) [arXiv:1706.07553 [hep-ph]].
- [24] M. S. Liu, F. X. Liu, X. H. Zhong and Q. Zhao, [arXiv:2006.11952 [hep-ph]].
- [25] B. D. Wan and C. F. Qiao, Phys. Lett. B **817**, 136339 (2021) [arXiv:2012.00454 [hep-ph]].
- [26] M. Karliner and J. L. Rosner, Phys. Rev. D **102**, no.11, 114039 (2020) [arXiv:2009.04429 [hep-ph]].
- [27] Q. F. Lü, D. Y. Chen and Y. B. Dong, Eur. Phys. J. C **80**, no.9, 871 (2020) [arXiv:2006.14445 [hep-ph]].
- [28] Z. R. Liang, X. Y. Wu and D. L. Yao, Phys. Rev. D **104**, no.3, 034034 (2021) [arXiv:2104.08589 [hep-ph]].
- [29] Q. Li, C. H. Chang, G. L. Wang and T. Wang, Phys. Rev. D **104**, no.1, 014018 (2021) [arXiv:2104.12372 [hep-ph]].
- [30] H. W. Ke, X. Han, X. H. Liu and Y. L. Shi, Eur. Phys. J. C **81**, no.5, 427 (2021) [arXiv:2103.13140 [hep-ph]].
- [31] M. A. Bedolla, J. Ferretti, C. D. Roberts and E. Santopinto, Eur. Phys. J. C **80**, no.11, 1004 (2020) [arXiv:1911.00960 [hep-ph]].
- [32] R. Zhu, Nucl. Phys. B **966**, 115393 (2021) [arXiv:2010.09082 [hep-ph]].
- [33] E. Fermi, Z. Phys. **29**, 315-327 (1924)
- [34] E. J. Williams, Phys. Rev. **45**, 729-730 (1934)
- [35] C. F. von Weizsacker, Z. Phys. **88**, 612-625 (1934)
- [36] V. M. Budnev, I. F. Ginzburg, G. V. Meledin and V. G. Serbo, Phys. Rept. **15**, 181-281 (1975)
- [37] C. A. Bertulani and G. Baur, Phys. Rept. **163**, 299 (1988)
- [38] G. Baur, K. Hencken, D. Trautmann, S. Sadovskiy and Y. Kharlov, Phys. Rept. **364**, 359-450 (2002) [arXiv:hep-ph/0112211 [hep-ph]].
- [39] C. A. Bertulani, S. R. Klein and J. Nystrand, Ann. Rev. Nucl. Part. Sci. **55**, 271-310 (2005) [arXiv:nucl-ex/0502005 [nucl-ex]].
- [40] G. Baur, K. Hencken and D. Trautmann, Phys. Rept. **453**, 1-27 (2007) [arXiv:0706.0654 [nucl-th]].
- [41] A. J. Baltz, G. Baur, D. d'Enterria, L. Frankfurt, F. Gelis, V. Guzey, K. Hencken, Y. Kharlov, M. Klasen and S. R. Klein, *et al.* Phys. Rept. **458**, 1-171 (2008) [arXiv:0706.3356 [nucl-ex]].
- [42] S. Klein and P. Steinberg, Ann. Rev. Nucl. Part. Sci. **70**, 323-354 (2020) doi:10.1146/annurev-nucl-030320-033923 [arXiv:2005.01872 [nucl-ex]].
- [43] W. Zha, L. Ruan, Z. Tang, Z. Xu and S. Yang, Phys. Lett. B **781**, 182-186 (2018) doi:10.1016/j.physletb.2018.04.006 [arXiv:1804.01813 [hep-ph]].
- [44] S. R. Klein, Phys. Rev. C **97**, no.5, 054903 (2018) doi:10.1103/PhysRevC.97.054903 [arXiv:1801.04320 [nucl-th]].
- [45] C. Azevedo, V. P. Gonçalves and B. D. Moreira, Eur. Phys. J. C **79**, no.5, 432 (2019) [arXiv:1902.00268 [hep-ph]].
- [46] S. Klein, A. H. Mueller, B. W. Xiao and F. Yuan, Phys. Rev. D **102**, no.9, 094013 (2020) [arXiv:2003.02947 [hep-ph]].
- [47] B. W. Xiao, F. Yuan and J. Zhou, Phys. Rev. Lett. **125**, no.23, 232301 (2020) doi:10.1103/PhysRevLett.125.232301 [arXiv:2003.06352 [hep-ph]].
- [48] J. D. Brandenburg, W. Zha and Z. Xu, Eur. Phys. J. A **57**, no.10, 299 (2021) [arXiv:2103.16623 [hep-ph]].
- [49] J. Adams *et al.* [STAR], Phys. Rev. C **70**, 031902 (2004) doi:10.1103/PhysRevC.70.031902 [arXiv:nucl-ex/0404012 [nucl-ex]].
- [50] J. Adam *et al.* [STAR], Phys. Rev. Lett. **121**, no.13, 132301 (2018) [arXiv:1806.02295 [hep-ex]].
- [51] J. Adam *et al.* [STAR], Phys. Rev. Lett. **127**, no.5, 052302 (2021) [arXiv:1910.12400 [nucl-ex]].
- [52] E. Abbas *et al.* [ALICE], Eur. Phys. J. C **73**, no.11, 2617 (2013) [arXiv:1305.1467 [nucl-ex]].
- [53] M. Aaboud *et al.* [ATLAS], Phys. Rev. Lett. **121**, no.21, 212301 (2018) doi:10.1103/PhysRevLett.121.212301 [arXiv:1806.08708 [nucl-ex]].
- [54] G. Aad *et al.* [ATLAS], Phys. Rev. C **104**, 024906 (2021) doi:10.1103/PhysRevC.104.024906 [arXiv:2011.12211 [nucl-ex]].
- [55] A. M. Sirunyan *et al.* [CMS], Phys. Rev. Lett. **127**, no.12, 122001 (2021) doi:10.1103/PhysRevLett.127.122001 [arXiv:2011.05239 [hep-ex]].
- [56] V. P. Gonçalves, D. T. Da Silva and W. K. Sauter, Phys. Rev. C **87**, no.2, 028201 (2013) [arXiv:1209.0701 [hep-ph]].
- [57] V. P. Gonçalves and M. M. Jaime, Phys. Lett. B **805**, 135447 (2020) [arXiv:1911.10886 [hep-ph]].
- [58] B. D. Moreira, C. A. Bertulani, V. P. Gonçalves and F. S. Navarra, Phys. Rev. D **94**, no.9, 094024 (2016) [arXiv:1610.06604 [hep-ph]].

- [59] V. P. Gonçalves and B. D. Moreira, Eur. Phys. J. C **79**, no.1, 7 (2019) [arXiv:1809.08125 [hep-ph]].
- [60] V. P. Gonçalves and B. D. Moreira, Phys. Lett. B **816**, 136249 (2021) [arXiv:2101.03798 [hep-ph]].
- [61] A. Esposito, C. A. Manzari, A. Pilloni and A. D. Polosa, Phys. Rev. D **104**, no.11, 114029 (2021) [arXiv:2109.10359 [hep-ph]].
- [62] M. Drees, J. R. Ellis and D. Zeppenfeld, Phys. Lett. B **223**, 454-460 (1989)
- [63] E. Papageorgiu, Phys. Lett. B **250**, 155-160 (1990)
- [64] J. Q. Zhu, Z. L. Ma, C. Y. Shi and Y. D. Li, Nucl. Phys. B **900**, 431-445 (2015)
- [65] D. d'Enterria, D. E. Martins and P. Rebello Teles, Phys. Rev. D **101**, no.3, 033009 (2020) [arXiv:1904.11936 [hep-ph]].
- [66] R. Bruce, D. d'Enterria, A. de Roeck, M. Drewes, G. R. Farrar, A. Giammanco, O. Gould, J. Hajer, L. Harland-Lang and J. Heisig, *et al.* J. Phys. G **47**, no.6, 060501 (2020) doi:10.1088/1361-6471/ab7ff7 [arXiv:1812.07688 [hep-ph]].
- [67] M. Aaboud *et al.* [ATLAS], Nature Phys. **13**, no.9, 852-858 (2017) doi:10.1038/nphys4208 [arXiv:1702.01625 [hep-ex]].
- [68] G. Aad *et al.* [ATLAS], JHEP **11**, 050 (2021) doi:10.1007/JHEP11(2021)050 [arXiv:2008.05355 [hep-ex]].
- [69] A. M. Sirunyan *et al.* [CMS], Phys. Lett. B **797**, 134826 (2019) doi:10.1016/j.physletb.2019.134826 [arXiv:1810.04602 [hep-ex]].
- [70] M. Vidovic, M. Greiner, C. Best and G. Soff, Phys. Rev. C **47**, 2308-2319 (1993)
- [71] W. Zha, J. D. Brandenburg, Z. Tang and Z. Xu, Phys. Lett. B **800**, 135089 (2020) doi:10.1016/j.physletb.2019.135089 [arXiv:1812.02820 [nucl-th]].
- [72] R. J. Wang, S. Pu and Q. Wang, Phys. Rev. D **104**, no.5, 056011 (2021) doi:10.1103/PhysRevD.104.056011 [arXiv:2106.05462 [hep-ph]].
- [73] M. Klusek-Gawenda, W. Schäfer and A. Szczurek, Phys. Lett. B **814**, 136114 (2021) [arXiv:2012.11973 [hep-ph]].
- [74] C. Li, J. Zhou and Y. J. Zhou, Phys. Lett. B **795**, 576-580 (2019) [arXiv:1903.10084 [hep-ph]].
- [75] C. Li, J. Zhou and Y. J. Zhou, Phys. Rev. D **101**, no.3, 034015 (2020) [arXiv:1911.00237 [hep-ph]].
- [76] R. D. Woods and D. S. Saxon, Phys. Rev. **95**, 577-578 (1954)
- [77] S. Klein and J. Nystrand, Phys. Rev. C **60**, 014903 (1999) [arXiv:hep-ph/9902259 [hep-ph]].
- [78] G. Baur, K. Hencken and D. Trautmann, J. Phys. G **24**, 1657-1692 (1998) [arXiv:hep-ph/9804348 [hep-ph]].
- [79] K. T. R. Davies and J. R. Nix, Phys. Rev. C **14**, 1977-1994 (1976)
- [80] H. De Vries, C. W. De Jager and C. De Vries, Atom. Data Nucl. Data Tabl. **36**, 495-536 (1987)
- [81] Q. Y. Shou, Y. G. Ma, P. Sorensen, A. H. Tang, F. Videbæk and H. Wang, Phys. Lett. B **749**, 215-220 (2015) [arXiv:1409.8375 [nucl-th]].
- [82] C. N. Yang, Phys. Rev. **77**, 242-245 (1950)
- [83] S. R. Klein, J. Nystrand, J. Seger, Y. Gorbunov and J. Butterworth, Comput. Phys. Commun. **212**, 258-268 (2017) [arXiv:1607.03838 [hep-ph]].